HYDROLOGICAL PROCESSES
Hydrol. Process. **22**, 4783–4788 (2008)
Published online 17 July 2008 in Wiley InterScience
(www.interscience.wiley.com) DOI: 10.1002/hyp.7092

Modeling changes in rill erodibility and critical shear stress on native surface roads

Randy B. Foltz,[1]*† Hakjun Rhee[2] and William J. Elliot[1]†
[1] *USDA Forest Service Rocky Mountain Research Station, Moscow, ID, USA*
[2] *Department of Biological Systems Engineering, Washington State University, Pullman, WA, USA*

Abstract:

This study investigated the effect of cumulative overland flow on rill erodibility and critical shear stress on native surface roads in central Idaho. Rill erodibility decreased exponentially with increasing cumulative overland flow depth; however, critical shear stress did not change. The study demonstrated that road erodibility on the studied road changes over the course of one or more consecutive overland flow events. Therefore, model simulations that fail to take into consideration this change will probably over-estimate sediment yields. An exponential function describing the relationship between rill erodibility and cumulative overland flow depth is presented as a basis for future model development for simulating erosion on native surface roads. Copyright © 2008 John Wiley & Sons, Ltd.

KEY WORDS soil erosion; forestry; sediment depletion; overland flow; simulation; Idaho

Received 17 January 2008; Accepted 9 May 2008

INTRODUCTION

Forest roads are considered a significant source of sediment delivery in forested watersheds (Hoover, 1952; Weitzman and Trimble, 1955; Megahan and Kidd, 1972; Best *et al*., 1995; Motha *et al*., 2003). Forest roads located adjacent to streams and rivers can introduce sediment into the aquatic systems. A negative relationship between road density and fish population was reported (Lee *et al*., 1997; Thompson and Lee, 2000). It is important to thoroughly understand forest road erosion processes and to develop models that simulate the processes accurately so that forestland managers can evaluate the impacts of forest roads on erosion and sediment delivery.

There are many forest road erosion models, e.g. the Water Erosion Prediction Project (WEPP) model (Flanagan and Livingston, 1995), which assume constant/static soil erosion parameters, and thus constant erosion rates during overland flow events. However, sediment concentration from the road surface was reported to decrease during a single rainfall or overland flow event. Foltz (1993) reported that the ratio of initial sediment concentration to final sediment concentration decreased by a factor of two to four on native surface roads with wheel ruts, as seen in Figure 1; Coker *et al*. (1993) reported that the same ratio decreased by a factor of three on a freshly graded road surface; Ziegler *et al*. (2001b) reported a ratio decrease of three on unpaved mountain roads; and Croke *et al*. (2006) reported a ratio decrease of two on unsealed main and feeder access roads. The low sediment concentrations at the end of one overland flow event can carry over to subsequent events if the time between storms is short, i.e. less than a day; however, low sediment concentrations were not observed to carry over if the time between overland flow events was on the order of weeks (Foltz, 1993). These studies suggest that the sediment supply is depleted by rainfall events then becomes replenished over a period of days to weeks.

There can be many processes to replenish the sediment supply between runoff events on native surface roads. Previous studies (Coker *et al*., 1993; Ziegler *et al*., 2001b) indicated that traffic replenished the sediment supply by detaching fine particles from compacted road surface and/or generating surface fines from breaking down large particles into transportable small sizes. Based on field observation (Foltz, 1993), another process can be postulated: *road surface drying*. Drying of road surface consequently makes loose fines available for erosion. Solar energy input and evaporation are thought to be responsible for the surface drying.

Even though the decrease in sedimentation concentrations during a storm is widely known, there are few models that attempt to describe the depletion and replenishment of the sediment supply. Foltz (1993) proposed modifications to a riverbed armoring model (Borah *et al*., 1982) for shallow, concentrated flow in wheel ruts. When armoring occurs, the fine particles are washed away, leaving a less erodible surface that may be mobilized at a higher flow rate. Foltz's modified armoring model used an excess shear erosion model (Foster *et al*., 1995), and was able to predict wheel rut erosion within ±50% on roads when mean particle diameters were in the sand size

* Correspondence to: Randy B. Foltz, USDA Forest Service Rocky Mountain Research Station, 1221 S. Main St., Moscow, ID 83843, USA. E-mail: rfoltz@fs.fed.us
† The contributions of Randy B. Foltz and William J. Elliot to this article were prepared as part of their official duties as United States Federal Government employees.

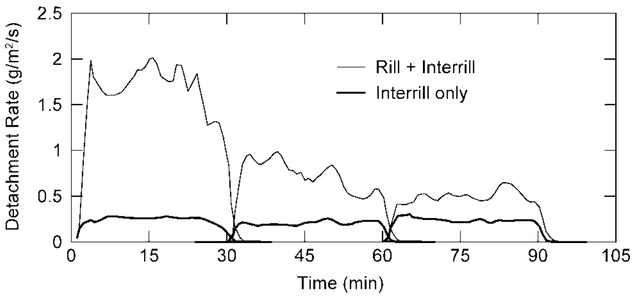

Figure 1. Runoff and detachment rate from native surface road (Foltz and Burroughs, 1990). Detachment rate from interrill erosion did not change, but detachment rate from rill and interrill erosion decreased with three consecutive rainfall events

range. For road surfacing with mean diameters in the silt range, the model was less well suited and simple correlations between sediment rate and overland flow rate were suggested (Foltz, 1993).

Depletion and replenishment of the sediment supply after the flush by runoff events was studied by Ziegler *et al.* (2000a,b; 2001a,b; 2002). They explained the regeneration of loose sediment between and during storms in terms of 'surface preparation' (cf. Bryan, 1996), a term referring to any process influencing the availability, erodibility/detachability or transport of road surface material: e.g. traffic, road maintenance, and mass wasting processes. Sediment transport on unpaved mountain roads was modelled using KINEROS2, in which the sediment transport algorithm was coupled to an empirical exponential decay function that was based on the disturbed surface erosion model of Megahan (1974). Ziegler *et al.*'s approach treated splash and hydraulic erosion on roads as dynamic processes (Ziegler *et al.*, 2000a). The approach, however, failed to simulate high initial flushes of loose road surface sediment, suggesting that additional calibration using data from road surfaces representing a greater range of loose surface material was needed (Ziegler *et al*, 2002). Nevertheless, the dynamic erosion approach was a substantial improvement over simulations performed with erodibility remaining static.

An approach to investigating the depletion and replenishment processes of sediment supply is to identify the process based on field observations/experiments, to develop a model, and to parameterize it using field experiments. The erosion process can be explicitly divided into interrill and rill erosion based on the transport mechanism of the eroded sediment (Foster and Meyer, 1975; Meyer *et al.*, 1975). Interrill erosion includes raindrop splash and erosion from shallow overland flow, and rill erosion is the detachment and transport of soil by a concentrated flow of water (Elliot and Ward, 1995). Interrill erodibility is the model parameter for interrill erosion, and rill erodibility and critical shear stress are model parameters for rill erosion. These three soil parameters are affected by soil properties, and vary widely among soils (Laflen *et al.*, 1991). They are also critical input parameters for process-based erosion models.

Figure 1, based on Foltz and Burroughs (1990), illustrates rill and interrill erosion processes on a native surface road. In their study, three 30-min simulated rainfalls of 50 mm h^{-1} intensity were applied to the paired 1·52 m × 30·5 m plots: rill plus interrill and interrill only plots. The rill plus interrill plots included a wheel rut and an overland flow area; therefore, sediment was from rill and interrill erosion. The interrill only plots contained an overland flow area without a wheel rut; therefore, sediment was from interrill erosion. The simulated rainfall experiments on these plots showed that interrill erosion rate didn't change during constant simulated rainfall events; however, rill erosion rate decreased (Foltz and Burroughs, 1990; Foltz, 1993).

The objectives of this paper are (1) to determine changes in rill erosion parameters during simulated overland flow events, and (2) to develop mathematical equations that describe these changes. Once developed, the mathematical equations can be used for further development and parameterization of a sediment depletion and replenishment model. The replenishment of the sediment supply is beyond the scope of this study.

RILL EROSION MODEL

A widely used rill erosion model is based on detachment rate (D_r, $ML^{-2}T^{-1}$) (Foster *et al.*, 1977):

$$D_r = D_c \cdot \left(1 - \frac{G}{T_c}\right) \tag{1}$$

where D_c is detachment capacity of the flow ($ML^{-2}T^{-1}$), G is sediment load per unit width ($ML^{-2}T^{-1}$), and T_c is transport capacity of the flow ($ML^{-2}T^{-1}$), i.e., the maximum sediment load that the flow can carry in a given hydraulic condition. The sediment load (G) ranges from zero for water without sediment to the transport capacity. At transport capacity the term $(1 - G/T_c)$ equals zero, and the detachment rate is, therefore, zero.

Detachment capacity (D_c) is represented by the following excess shear erosion equation (Foster *et al.*, 1995):

$$D_c = K_r \cdot (\tau - \tau_c) \tag{2}$$

where K_r is the rill erodibility parameter (TL^{-1}), τ is hydraulic shear stress in the rill (FL^{-2}), and τ_c is critical shear stress required for detachment to occur (FL^{-2}). Critical shear stress is often thought of as the minimum hydraulic shear stress required to initiate sediment movement (Van Klaveren and McCool, 1998). The hydraulic shear stress is calculated as follows (Foster *et al.*, 1984):

$$\tau = \gamma \cdot R \cdot S_f \tag{3}$$

where γ is specific weight of water (FL^{-3}), R is hydraulic radius (L), and S_f is friction slope (L/L).

According to Equations (1) and (2), K_r and τ_c can be calculated if the detachment rate, shear stress, and initial sediment load are known. If water without sediment is introduced to the rill bed, $G = 0$ and the term

$(1 - G/T_c) = 1$, simplifying the equations to result in Equation (4) (Cochrane and Flanagan, 1997):

$$D_c = K_r \cdot (\tau - \tau_c) \tag{4}$$

For agricultural soil conditions where sediment supply is large and sediment depletion is infrequent, constant values for K_r and τ_c are adequate to characterize the sediment concentrations. For native surface roads, a detachment rate calculated from constant values for K_r and τ_c will not properly characterize the changing detachment rate as seen in Figure 1. Either K_r or τ_c, or both change with time during overland flow events.

METHODS

Study area

The Spruce Creek timber sale roads are located (44°40′N, 115°52′E) at 2000–2100 m elevation within the Payette National Forest, approximately 15 km east of Idaho State Highway 55 north of Cascade, Idaho. The road was constructed 2 years prior to the study and received only light weight, occasional administrative traffic after construction and prior to the study. The dominant soil parent material was decomposed granite. The soil of the running surface for this study was gravelly loamy sand (20% gravel, 64% sand, 14% silt, and 2% clay) with a mean diameter of 0·52 mm. The local climate was dry in the summer (about 10% of annual precipitation of 790 mm) and wet in winter (about 45% of annual precipitation).

Overland flow simulations

Overland flow simulations were conducted on fifteen 8 m bordered plots that were 0·25 m wide, which is the width of a typical single axle wheel rut. Surface organic materials (e.g. pine needles) were removed from the plots before overland flow simulations. No significant wheel tracks or rills were observed on the plots. To prevent water from flowing under the plot border, 2-inch L-shaped steel angle iron borders were placed parallel to the road gradient and attached to the road surface by a hammer and nails. Sediment-free water was introduced at the uphill end of each plot with a flow rate controller. The downhill end of the plots had a galvanized metal collector with a free overfall, where timed overland flow grab-samples were taken every minute. Half of the samples were used to determine flow rates. The other half were oven-dried at 105 °C to determine sediment concentrations. Sample volumes were adjusted based on the sediment concentration determined in the laboratory. Detachment rates were calculated from flow rates and sediment concentrations. To calculate the flow velocity, the time required for a slug of salt-laden dye to traverse the middle 3 m of the 8 m long plot was measured every 3 min using two conductivity meters, which recorded at 0·1 s intervals.

Three different flow rates (Low, 206 mL s^{-1}; Med, 413 mL s^{-1}; and High, 826 mL s^{-1}) were applied. These rates correspond to the runoff in a single 30 m long wheel rut from 12, 25 and 50 mm h^{-1} rainfall. Each flow rate was applied three times in the sequence of Low1, Med1, High1, Low2, Med2, High2, Low3, Med3, and High3. Each rate was applied for 3 min, with no time delay between each phase for a total simulation time of 27 min.

Rill erodibility and critical shear stress equations

To solve for K_r and τ_c in Equation (4), three values of detachment rate (D_r) and hydraulic shear stress (τ) were required from three flow rates (Low, Med, and High). The slope of D_r versus τ equals K_r and the x-axis intercept is τ_c (Cochrane and Flanagan, 1997).

The rill erodibility parameter K_r is often thought of as a measure of the soil's susceptibility to rilling (Foster *et al*, 1977). Since a larger K_r indicates a more erosion-prone soil, we hypothesized that K_r should decrease during an overland flow event. Previous study results from Megahan (1974), Coker *et al*. (1993), Foltz (1993), and Ziegler *et al*. (2000a,b; 2001a,b; 2002) suggested that sediment concentration decreased in an exponential manner during overland flow events. Therefore, either K_r should decrease in an exponential manner or τ_c should increase in an exponential manner during overland flow events as a function of cumulative overland flow depth. Equation (5) illustrates this relationship for K_r.

$$K_r = A \cdot e^{-\frac{d}{d_0}} \tag{5}$$

where A is a regression constant, d is cumulative flow depth, and d_0 is a regression constant.

As the flow removes smaller particles, the shear stress required to move the remaining coarser particles was expected to increase. This corresponds to an increase in critical shear stress during the overland flow event. It was hypothesized that τ_c should increase in an exponential manner with cumulative overland flow depth (d), as shown in Equation (6).

$$\tau_c = A \cdot e^{\frac{d}{d_0}} \tag{6}$$

Data analysis

An ANOVA test was used to determine if there was a significant change in K_r and τ_c during overland flow events. If an ANOVA test indicated a significant difference, Tukey's HSD test (honestly significant difference test; Tukey, 1953) was used to identify differences among the flow sequences. The relationship between K_r and d was then determined using Equation (5) and the relationship between τ_c and d using Equation (6) after logarithmic-transformation of data.

RESULTS

Overland flow and sediment concentration

Figure 2 shows a typical hydrograph and detachment rate graph. The detachment rate started low and increased

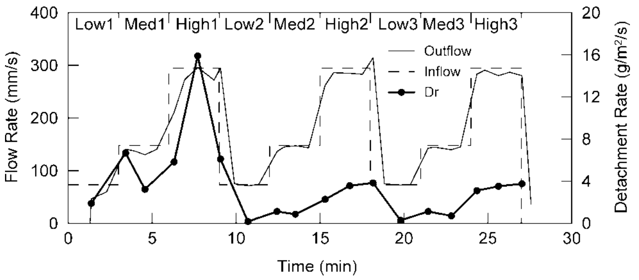

Figure 2. Hydrograph and detachment rate from plot 7 (Table I) showing three flows repeated three times

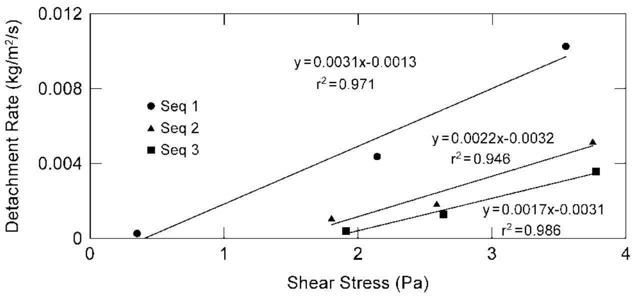

Figure 3. Typical plot (plot 8 from Table I) of shear stress versus detachment rate. Flow sequence 1 has steeper slope (K_r) and smaller X-intercept (τ_c) than flow sequence 2 and 3

during the Low1 flow. During the Med1 flow, twice the Low1 rate, the sediment concentration again spiked and subsequently declined. During the highest flow rate (High1), twice the Med1 and four times the Low1 rate, the sediment concentration spiked and subsequently declined.

Changes in rill erodibility and critical shear stress

Figure 3 shows three regression lines used to determine rill erodibility and critical shear stress for a set of flow sequences. Note that the steepest slope, i.e. the highest K_r, occurred from the first flow set and that K_r decreased after the first flow set. Also note that the x-axis intercept increased with additional flow sets.

From the 15 plots there were 45 possible K_r and τ_c pairs. A total of 31 pairs met the acceptance criteria of having positive K_r and τ_c values derived from three flows. These 31 pairs were used in the subsequent analysis as seen in Table I.

The calculated values of K_r are shown in Table I, and plotted on a semi-logarithmic scale in Figure 4. As expected the values started high and decreased with increasing cumulative overland flow depth. The K_r values ranged from $0{\cdot}494 \times 10^{-3}$s m^{-1} to $7{\cdot}55 \times 10^{-3}$s m^{-1} and are summarized in Table II. An ANOVA test showed that the sequence of flows made a statistically significant difference in K_r (P-value $< 0{\cdot}001$). Tukey's HSD test showed that the K_r values of flow sequence 1 were larger than flow sequence 2 and 3; and there was no difference between flow sequence 2 and 3.

The relationship between rill erodibility and cumulative flow depth was determined as follows:

$$K_r = 3{\cdot}80 \times 10^{-3} \cdot e^{-\frac{d}{192}} \qquad (7)$$

where K_r is rill erodibility (s m^{-1}), and d is cumulative flow depth (mm). The P-value for this equation was 0·0027, and the coefficient of determination (r^2) was 0·271.

The calculated values of τ_c are shown in Table I, and plotted in Figure 5. The τ_c values ranged from 0·41 Pa to 2·55 Pa and are summarized in Table II. An ANOVA test showed that the sequence of flows did not make a statistically significant difference in τ_c (P-value of 0·099).

Table I. Calculated rill erodibility (K_r) and critical shear stress (τ_c) during overland flow simulations. Only positive K_r and τ_c values are shown

Flow sequence	Plot number	Cumulative flow depth (mm)	K_r (10^{-3}s m^{-1})	τ_c (Pa)	r^2
1	1	63·3	3·23	1·82	0·99+
1	5	61·9	7·55	1·31	0·99
1	7	74·5	5·65	1·45	0·98
1	8	65·1	3·09	0·41	0·97
1	9	63·0	1·27	0·69	0·55
1	10	74·1	5·14	0·52	0·76
2	1	147·3	0·49	0·69	0·99
2	2	150·5	0·96	1·11	0·94
2	3	112·0	1·85	0·47	0·98
2	4	171·6	0·62	0·88	0·89
2	5	151·3	2·52	1·10	0·94
2	6	164·5	0·66	1·26	0·61
2	7	168·8	1·79	1·59	0·93
2	8	159·1	2·16	1·47	0·95
2	9	152·8	0·97	1·53	0·88
2	10	171·0	0·98	0·88	0·99+
2	11	169·1	2·62	0·65	0·99+
2	15	163·0	1·82	0·56	0·99
3	1	234·6	0·66	1·84	0·95
3	2	234·3	1·98	1·46	0·91
3	3	210·7	0·59	0·71	0·99
3	4	270·3	0·69	1·64	0·98
3	5	242·7	2·70	1·85	0·99+
3	6	259·1	0·93	2·55	0·94
3	7	263·7	1·87	1·86	0·99+
3	8	250·5	1·73	1·77	0·99
3	9	245·9	1·01	2·46	0·96
3	10	270·3	0·53	1·03	0·91
3	11	266·6	1·38	0·57	0·45
3	14	267·2	2·18	0·78	0·81
3	15	255·9	0·85	0·67	0·99+

Table II. Summary of changes in rill erodibility (K_r) and critical shear stress (τ_c) across flow sequences during overland flow simulations

Flow sequence	Number of observations[a]	K_r (10^{-3}s m^{-1})			τ_c (Pa)		
		Mean	Stdev	CV[b]	Mean	Stdev	CV
1	6	4·32	2·23	51·6	1·03	0·571	55·3
2	12	1·45	0·760	52·3	1·02	0·389	38·3
3	13	1·31	0·709	54·0	1·48	0·671	45·4

[a] Observation number varies because 'events' where either K_r or τ_c was negative were excluded.
[b] CV is the coefficient of variation.

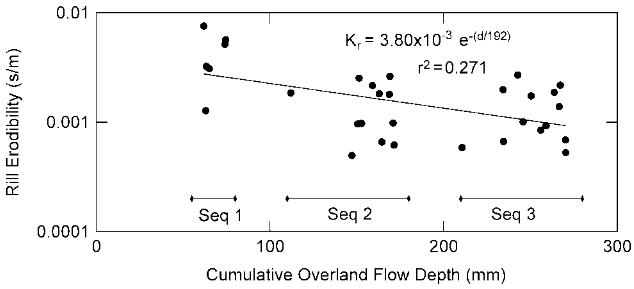

Figure 4. Observed and predicted rill erodibility change during overland flow events. Rill erodibility decreased exponentially with increasing cumulative overland flow depth

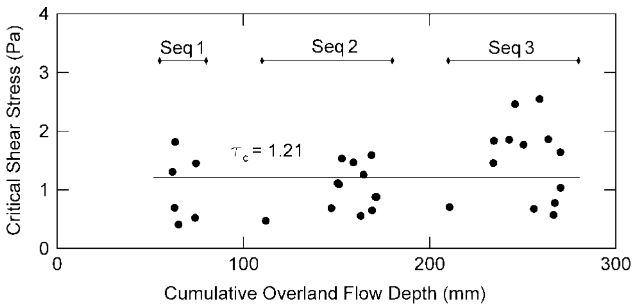

Figure 5. Observed critical shear stress change during overland flow events. Critical shear stress did not change with increasing cumulative overland flow depth

Therefore, sediment depletion on road surface had no statistically significant effect on τ_c.

DISCUSSION

From the 15 plots and 45 possible K_r and τ_c pairs, 31 pairs had both positive K_r and τ_c values; 14 pairs were dropped from data analysis. Two of them were from field simulation failures and 12 from negative values of K_r or τ_c. There were eight negative values of K_r or τ_c from sequence 1, two negative values from sequence 2, and two negative values from sequence 3; therefore, there were more negative values of K_r or τ_c in sequence 1 than sequence 2 and 3 by a factor of four. This trend in negative values of K_r or τ_c is speculated to arise as follows: (1) for the initial flow (Low1), infiltration rate is high, and a portion of the inflow is lost by infiltration. Figure 2 shows that outflow rate is much lower than inflow rate in Low1. (2) A greater variation in loose sediment quantity might exist among the plots before flow sequence 1. Different levels of sediment replenishment (surface preparation) occurred at different plot locations before the simulations. Similar difficulties in simulating initial flushes of loose sediment were reported by Ziegler *et al.* (2002). (3) If sediment supply is plentiful before the simulations, erosion in Low1 may be *transport-limited*. The excess shear erosion model (Equation (2)) was developed and is applicable for *detachment-limited* erosion conditions, and does not properly represent the transport-limited process.

This study investigated an approach to modelling dynamic erosion in native surface roads. An improvement was made to the dynamic erosion model of Ziegler *et al.* (2000a,b; 2001a,b; 2002). They explicitly separated the dynamic erosion process into splash and hydraulic erosion, whereas the focus of this study was changes in rill erosion.

CONCLUSIONS

Overland flow simulations on 8 m long plots on forest roads in central Idaho were used to determine changes in rill erosion parameters during simulated overland flow events. The study results demonstrated that rill erodibility decreased exponentially with increasing cumulative flow depth; however, critical shear stress did not change. A mathematical equation was developed to describe this change in rill erodibility as a dynamic property that can change during a single runoff event. Existing erosion models assume constant erodibility parameter values. The implication is that over-prediction of sediment yields would probably result if constant rill erodibility values are used when modeling road surface erosion from consecutive runoff events. The results from this study provide a methodology to model sediment depletion on native surface roads. Coupled with further studies on the replenishment of sediment supply, rill erodibility changes can be incorporated into existing process-based models and used to improve the accuracy of forest road erosion models.

REFERENCES

Best DW, Kelsey HM, Hagans DK, Alpert M. 1995. Role of fluvial hillslope erosion and road construction in the sediment budget of Garrett Creek, Humboldt County, California. In *Geomorphic Processes and Aquatic Habitat in the Redwood Creek Basin, Northwestern California*, Nolan KM, Kelsey HM, Marron DC (eds). USGS Professional Paper 1454. USGS: Washington, DC; M1–9.

Borah DK, Alonso CV, Prasad SN. 1982. Routing graded sediments in streams: Formulations. *Journal of the Hydraulics Division, ASCE* **108**(HY12): 1486–1503.

Bryan RB. 1996. Erosion response to variations in interstorm weathering conditions. In *Advances in Hillslope Processes*, Vol. 1, Anderson MG, Brooks SM (eds). John Wiley & Sons: Chichester; 589–612.

Cochrane TA, Flanagan DC. 1997. Detachment in a simulated rill. *Transactions of the ASAE* **40**(1): 111–119.

Coker RJ, Fahey BD, Payne JJ. 1993. Fine sediment production from truck traffic, Queen Charlotte Forest, Marlborough Sounds, New Zealand. *Journal of Hydrology (NZ)* **31**(1): 56–64.

Croke J, Mockler S, Hairsine P, Fogarty P. 2006. Relative contributions of runoff and sediment from sources within a road prism and implications for total sediment delivery. *Earth Surface Processes and Landforms* **31**: 457–468. DOI: 10·1002/esp.1279.

Elliot WE, Ward AD. 1995. Soil erosion and control practices. In *Environmental Hydrology*, Ward AD, Elliot WJ (eds). CRC Press: Boca Raton, Florida; 177–204.

Flanagan DC, Livingston SJ, eds. 1995. *WEPP User Summary*. NSERL Report No. 11. USDA-Agricultural Research Service, National Soil Erosion Research Laboratory: W. Lafayette, IN.

Foltz RB. 1993. *Sediment processes in wheel ruts on unsurfaced forest roads*. PhD dissertation, University of Idaho, Department of Civil Engineering, Moscow, ID.

Foltz RB, Burroughs ER. 1990. Sediment production from forest roads with wheel ruts. In *Proceedings from Watershed Planning and Analysis in Action*, ASCE, Durango, CO, July 9–11, 1990. ASCE: Reston, VA; 266–275.

Foster GR, Meyer LD. 1975. Mathematical simulation of upland erosion using fundamental erosion mechanics. In *Present and Prospective*

Technology for Predicting Sediment Yields and Sources: Proceedings of the 1972 Sediment-Yield Workshop, USDA Sedimentation Laboratory, Oxford, MS, 28–30 November, 1972. ARS-S-40. USDA-Agricultural Research Service: Washington, DC; 190–207.

Foster GR, Meyer LD, Onstad CA. 1977. An erosion equation derived from basic principles. *Transactions of the ASAE* **20**(4): 678–682.

Foster GR, Huggins LF, Meyer LD. 1984. A laboratory study of rill hydraulics: II. Shear stress relationships. *Transactions of the ASAE* **27**(3): 797–804.

Foster GR, Flanagan DC, Nearing MA, Lane LJ, Risse LM, Finkner SC. 1995. Hillslope erosion component. In *USDA-Water Erosion prediction Project, Hillslope Profile and Watershed Model Documentation*, Flanagan DC, Nearing MA (eds). NSERL Report No. 10. USDA-Agricultural Research Service, National Soil Erosion Research Laboratory: W. Lafayette, IN.

Hoover MD. 1952. Water and timber management. *Journal of Soil and Water Conservation* **7**(2): 75–78.

Laflen JM, Elliot WJ, Simanton JR, Holzhey CS, Kohl KD. 1991. WEPP: Soil erodibility experiments for rangeland and cropland soils. *Journal of Soil and Water Conservation* **46**(1): 39–44.

Lee DC, Sedell JR, Rieman BE, Thurow RF, Williams JE, Burns D, Clayton J, Decker L, Gresswell R, House R, Howell P, Lee KM, MacDonald K, McIntyre J, McKinney S, Noel T, O'Connor JE, Overton CK, Perkinson D, Tu K, Van Eimeren P. 1997. Broadscale assessment of aquatic species and habitats. In *An Assessment of Ecosystem Components in the Interior Columbia Basin and Portions of the Klamath and Great Basins: Volume III*, Quigley TM, Arbelbide SJ (eds). General Technical Report PNW-GTR-405. USDA Forest Service Pacific Northwest Research Station: Portland, OR; 1057–1713.

Megahan WF. 1974. *Erosion over Time on Severely Disturbed Granite Soils: A Model.* USDA–Forest Service Research Paper INT-156. Intermountain Research Station: Ogden, UT.

Megahan WF, Kidd WJ. 1972. Effects of logging and logging roads on erosion and sediment deposition form steep terrain. *Journal of Forestry* **70**(3): 136–141.

Meyer LD, Foster GR, Romkens MJM. 1975. Origin of eroded soil from upland slopes. In *Present and Prospective Technology for Predicting Sediment Yields and Sources: Proceedings of the 1972 Sediment-Yield Workshop*, USDA Sedimentation Laboratory, Oxford, MS, 28–30 November, 1972. ARS-S-40. USDA-Agricultural Research Service: Washington, DC; 177–189.

Motha JA, Wallbrink PJ, Hairsine PB, Grayson RB. 2003. Determining the sources of suspended sediment in a forested catchment in south-eastern Australia. *Water Resources Research* **39**(3): ESG2-1–ESG2-14. DOI: 10·1029/2001WR000794.

Thompson WL, Lee DC. 2000. Modeling relationships between landscape-level attributes and snorkel counts of chinook salmon and steelhead parr in Idaho. *Canadian Journal of Fisheries and Aquatic Sciences* **57**(9): 1834–1842.

Tukey JW. 1953. The problem of multiple comparisons. Unpublished manuscript. Princeton University, Department of Statistics, Princeton, NJ.

Van Klaveren RW, McCool DK. 1998. Erodibility and critical shear of a previously frozen soil. *Transactions of the ASAE* **41**(5): 1315–1321.

Weitzman S, Trimble GR. 1955. Integrating timber and watershed management in mountain areas. *Journal of Soil and Water Conservation* **10**(2): 70–75.

Ziegler AD, Sutherland RA, Giambelluca TW. 2000a. Partitioning total erosion on unpaved roads into splash and hydraulic components: The roles of interstorm surface preparation and dynamic erodibility. *Water Resources Research* **36**(9): 2787–2791.

Ziegler AD, Sutherland RA, Giambelluca TW. 2000b. Runoff generation and sediment production on unpaved roads, footpaths and agricultural land surfaces in northern Thailand. *Earth Surfaces and Landforms* **25**(5): 519–534.

Ziegler AD, Giambelluca TW, Sutherland RA. 2001a. Erosion prediction on unpaved mountain roads in northern Thailand: validation of dynamic erodibility modeling using KINEROS2. *Hydrological Processes* **15**(3): 337–358.

Ziegler AD, Sutherland RA, Giambelluca TW. 2001b. Interstorm surface preparation and sediment detachment by vehicle traffic on unpaved mountain roads. *Earth Surface Processes and Landforms* **26**(3): 235–250.

Ziegler AD, Giambelluca TW, Sutherland RA. 2002. Improved method for modeling sediment transport on unpaved roads using KINEROS2 and dynamic erodibility. *Hydrological Processes* **16**(15): 3079–3089. DOI:10·1002/hyp.1090.